RSC Advances

ROYAL SOCIETY OF CHEMISTRY

www.rsc.org/advances

Surface Molecular Imprinting on Silane-Functionalized Carbon Dots for Selective Recognition of Nifedipine

Roghayeh Jalili and Mohammad Amjadi*

Department of Analytical Chemistry, Faculty of Chemistry, University of Tabriz, Tabriz 5166616471, Iran

* Corresponding author

Email: amjadi@tabrizu.ac.ir

Tel: +984133393109; Fax: +984133340191

Abstract:

This paper describes the development of a novel eco-friendly molecularly imprinted fluorescent sensor for nifedipine (NIF) based on silane-functionalized carbon dots (MIP@SiC-dots). The sensor were synthesized by sol–gel reaction (imprinting process) and characterized by fluorescence spectroscopy, UV–vis spectroscopy, TEM, SEM and FT-IR. Fluorescence from the MIP@SiC-dots was more strongly quenched by NIF than that of the non-imprinted polymer, which indicated that the MIP-coated SiC-dots, acted as a fluorescence sensing material, could recognize NIF. Under optimized operational conditions, a linear response was obtained in the concentration range from 0.28 to 3.4 μM with a detection limit of 0.076 μM. The proposed sensor was applied to NIF determination in serum and urine samples with the recoveries from 94.2 to 105.6%, showing a promising potential application in biomedical analysis.

Keywords: Carbon Dots; Molecularly imprinted polymer; Nifedipine; Fluorescence.

1. Introduction:

Nifedipine [1, 4-dihydro-2, 6-dimethyl-4-(2-nitrophenyl)-3, 5-pyridinedicarboxylic acid dimethyl ester], shown in Fig. 1(a), is a well-known dihydropyridine calcium antagonist, which retards the passage of calcium ions through membranes into cardiac and vascular smooth muscle cells. It causes coronary vasodilation and increases coronary blood flow and reduces the total peripheral vascular resistance. It is widely used in the treatment of hypertension angina pectoris, various other cardiovascular disorders and Reynaud's phenomenon. However, its overdose is toxic and may cause severe dizziness, pounding heartbeats, nausea and vomiting [1,2] Current analytical methods for nifedipine include Ultra-high-performance liquid chromatography[3] (UPLC), UPLC-MS/MS [4], voltammetry [5,6], and spectrometry [7].

Molecularly imprinted polymers are tailor-made synthetic receptors, prepared by co-polymerization of functional and crosslinking monomers in the presence of a molecular template. After removal of the template, binding sites are revealed that allow binding of the target molecule with a very high specificity and affinity [8]. Recently, the preparation of MIPs using sol-gel technology has drawn much attention. Molecularly imprinted sol-gel systems are inorganic polymers with rigid macropore frameworks that have specific recognition ability for template. Small inorganic and organic molecules can penetrate freely to these macropores, while the rigid physical structure can maintain its original properties when being treated by strong acid, strong base, or heat. Compared with acrylic polymer-based MIPs, the control of thickness, porosity, and surface area of sol-gel-based MIPs is easy, while the selectivity and diffusion are comparable or even better, making the sol-gel method suitable for the construction of electrochemical and optical sensors[9]. This kind of MIPs has been reported for enrofloxacin[10], 2-nonylphenol[11], salicylic acid [8], L-tyrosine [12], yeast cells [13] as templates.

Fluorescent carbon dots (C-dos), a fascinating class of quantum dots (QDs) based on carbon materials, have attracted increasing attention in recent years. Compared to traditional semiconductor QDs and organic dyes, C-dots are superior in terms of low toxicity, excellent biocompatibility, high stability and strong resistance to photodegradation, ease of synthesis and functionalization. C-dots are conjugated systems with a sp^2 hybridization and with different arrangements of the carbon sheets, ranging from highly disordered graphite to amorphous carbon [14,15]. Moreover, the surface of C-dots may have different functional groups, that can be obtained in situ, during the synthetic process themselves, or ex situ, in a second step under hard conditions [16–19]. In any case, the surface grafted chemical groups affect both the optical and the physico-chemical properties of these nanoparticles. Normally, to avoid low doping concentration, aggregation, or phase separation in the preparation of silica gel or polymer hybrid materials, C-dots are modified with organosilanes [20,21].

By combining the high selectivity of MIP and the efficient fluorescence properties of C-dots new methods for selective recognition and quantitative determination of target analytes can be developed. In such C-dot-based sensing systems fluorescence intensity changes when a target analyte binds to the imprinted cavities. It should be pointed out that semiconductor QDs coated with MIP film have been frequently reported [22–25] but MIP-capped C-dots for analytical applications are still in an early stage of development [26].

In this work, a highly selective surface molecularly imprinted polymer for nifedipine (NIF) was synthesized on the surface of silane functionalized carbon dots (SiC-dots) by a sol–gel process and an eco-friendly fluorescent sensor was constructed to selectively detect nifedipine based on this composite. The response of fluorescence intensity and the application capability of the

developed molecularly imprinted sensor were fully evaluated in a series of experiments and the possible mechanism was discussed.

2. Experimental

2.1. Apparatus

Fluorescence spectra were recorded using a Shimadzu RF-540 fluorescence spectrophotometer (Kyoto, Japan) equipped with a quartz cell (1 cm×1 cm). The slit widths of the excitation and emission monochromators were both set at 10 nm. UV-vis absorption spectra were obtained by a Cary-100 spectrophotometer (Varian, Sydney, Australia). All optical measurements were carried out under ambient temperature. The size and structure of SiC-dots and MIP@SiC-dots were characterized by Transmission electron microscopy (TEM) (BioTwin and CM 120, Philips, Netherlands) an d scanning electron microscope (SEM) (Mira 3 FEG, Tescan Co., Czech Republic). Fourier transform infrared (FT-IR) measurement was carried out with a Tensor-27 FT-IR spectrometer (Bruker Co., Germany).

2.2. Reagents and solutions

All reagents were of analytical grade and used as received. Doubly distilled de-ionized water obtained from Ghazi Serum Co. (Tabriz, Iran) was used for the preparation of all solutions. 3-aminopropyltriethoxysilane (APTES), trisodium citrate and nimodipine (NIM) were purchased from Merck (Darmstadt, Germany). Tetraethoxysilane (TEOS) was obtained from Sigma-Aldrich (US). Nifedipine was kindly provided by Dana Pharmaceutical Co (Tabriz, Iran) and a 1.0×10^{-3} mol L^{-1} standard stock solution was prepared in ethanol. This stock solution were kept in dark bottles immediately after preparation and stored at 4 °C. Working solutions were prepared daily by further dilution of the standard stock solution with water. These solutions were

also kept in dark bottles. Britton-Robinson buffer was prepared by mixing phosphoric acid (0.1 M), acetic acid (0.1 M) and boric acid (0.1 M). Buffer solutions were adjusted by adding the necessary amount of NaOH in order to obtain the appropriate pH.

2.3. Synthesis of SiC-dots

The *SiC-dots* were synthesized via a one-step hydrothermal method[27]. At first, 0.4 g trisodium citrate (carbon source) was dissolved in 8.0 mL deionized water into a three-necked flask, and degassed with nitrogen for 15 minutes. Then 2.0 mL of APTES (functionalization reagent) was injected into the nitrogen-saturated precursor solution and stirred for 10 min. The resultant precursor was sealed into a 50 mL Teflon equipped stainless steel autoclave followed by hydrothermal treatment at 200 °C for 2 h for carbonization of trisodium citrate and in situ surface functionalization. The color of the solution turned from colorless to yellow after this step. To remove the excess impurities at the end of the preparation, 1 kDa dialysis bag was used to purify the solution and the as-prepared SiC-dots solution was collected and stored at 4 °C for use.

2.4. Synthesis of MIP- and NIP-coated SiC-dots

The imprinting polymer were prepared by sol–gel procedure[28] at the surface of the SiC-dots. NIF template (30 mg) was dissolved in ethanol (20 mL) and mixed with APTES (60 μL). Then SiC-dots (2.0 mL) was added and the mixture was stirred for 10 min. Afterwards 100 μL of TEOS and 100 μL of ammonia aqueous solution (25%) were injected and the reaction system was sealed and kept under stirring in darkness at room temperature for 8 h. The resultant MIP-coated SiC-dots were centrifuged and washed with ethanol and distilled water. This step was repeated several times until no template was detected by UV–vis spectrophotometry. Finally, the obtained MIP-coated SiC-dots were re-dispersed in water and stored at 4 °C prior to use. The Non-

imprinted polymer coated SiC-dots (NIP@SiC-dots) as a control to evaluate the molecular recognition properties of imprinted materials was prepared using the same procedure but without addition of the template molecule.

2.5. Analytical procedure

To a 4.0-mL standard cuvette, 500 μL of stock solution of MIP@SiC- dots, 200 μL of Britton-Robinson buffer solution (pH=10, 0.1 M), and appropriate amounts of NIF solution were added and the volume was reached to 3.0 mL with deionized water. After incubation for 10 min, the fluorescence intensity was measured at 440 nm with an excitation wavelength of 360 nm.

2.6. Analysis of real samples

Human serum sample was obtained from Blood Transfusion Center (Tabriz, Iran). Urine sample was collected from a normal person. A 1.0-mL aliquot of serum or urine sample was placed into a centrifuge tube and spiked by adding appropriate volumes of NIF standard solution. Then, 2.0 mL of $Ba(OH)_2$ (0.1M) and 1.8 mL of $ZnSO_4$ (0.1M) were added into the tube in order to precipitate proteins. After centrifugation for 15 min, the clear supernatant was diluted to 20 mL and analyzed according to the general procedure.

3. Results and discussion

Silane-functionalized carbon dots (SiC-dots) were prepared by a simple one-pot hydrothermal approach as shown in Scheme 1. Figure 2a shows the transmission electron microscope (TEM) image of the prepared carbon dots, revealing that these carbon dots are well separated from each other and have a uniform dispersion without apparent aggregation and a relatively narrow size distribution between 3 and 7 nm. As demonstrated in Fig. 3, the prepared SiC-dots show an obvious absorption peak centered at 350 nm in the UV-Vis absorption spectrum. When excited

in the range of 320–380 nm, the SiC-dots exhibit an excitation-independent photoluminescence centered at 440 nm with a full width at half maximum (FWHM) as small as 50 nm (Fig. 3). The photoluminescence quantum yield obtained by using quinine sulphate as a standard[29] (54% in 0.1 M H_2SO_4) was found to be ~ 30%, which was believed to be high enough in sensor application. The FT-IR spectra of the C-dots are shown in Fig. S1 (Electronic Supplementary Material, ESM). The strong absorbance at 1388, and 3059 cm^{-1} are assigned to the N-H bending vibrations and the N- H stretching vibration, respectively. The stretching vibration of Si–O-CH (1035 cm^{-1}) and the asymmetric stretch of Si-CH_2 (756 cm^{-1}) arise from the APTES bonding on the surface of the C-dots. The peaks at 2933 and 1580 cm^{-1} demonstrated the presence of –CH2– and C=O, respectively.

3.2. Preparation and Characterization of MIP–coated C-dots

In this study, sol–gel process was adopted for the preparation of MIP on the surface of C-dots. In order to improve the interaction between C-dots and molecularly imprinted silica matrix, C-dots have to be coated with a layer of silica before the sol–gel hydrolysis and condensation imprinted polymerization reaction. The silica nanospheres were simply fabricated by means of the hydrolysis and condensation reaction of APTES and TEOS (cross-linker) in the presence of aqueous ammonia solution as the catalyst. In this nanosensor system, APTES plays two crucial roles: surface functionalization of C-dots and simultaneously acting as a functional monomer in the molecular imprinting process. NIF templates were assembled and immobilized into the matrix of silica by the silanization reaction between APTES and TEOS to form core-shell SiO_2@SiC-dots nanospheres. After the templates were extracted from the silica matrix by using solvent to decompose the hydrogen bond, the NIF-imprinted sites with the covalently anchored amino groups at the cavity were created in the silica matrix (Scheme 1).

The TEM image of MIP@SiC-dots observed is shown in Fig. 2b. From this image, the uniform regular spherical particle structure with an average diameter about 100 nm could be obviously observed, which verified the successful formation of a desired material shape and morphology. SEM results (Fig. 2c) provide further support for uniform structure and highly spherical morphology of MIP@SiC-dots.

FT-IR spectrum of MIP-coated QDs was shown in Fig.S2 (ESM). The strong and broad peak at 1000 to 1100 cm^{-1} indicates the Si–O–Si asymmetric stretching. The band at approximately 465 cm^{-1} was attributed to Si–O vibrations. The presence of band around 2900 cm^{-1} (aliphatic C-H stretching band) and broad absorption peaks at 3450 cm^{-1} and 1541 cm^{-1} (N-H band) suggests the existence of the aminopropyl group.

The imprinting factors (IF) of the imprinted polymers using different amounts of TEOS as cross-linkers were tested. The results (Fig. 4) indicated that the polymers that employed 100 μL of TEOS as the cross-linker have relatively better imprinting factor for NIF. The recognition sites may be wrapped in the internal region and the template may be not easy to be eluted by washing with a high cross-linking degree. Besides, polymers with a relatively low cross-linking degree may have a variable three dimensional structure which is unfavorable for rebinding. The amount of TEOS also affected the loading fractions of SiC-dots in silica shell, size of MIP@SiC-dots and fluorescence intensity.

The effect of APTES amount on the selectivity of MIP@SiC-dots was also investigated within the range of 10-100 μL (template and the cross-linker were kept constant at 30 mg and at100 μL, respectively). As shown in Fig. 5 optimum selectivity (IF) was obtained with 60 μL of APTES. Above this value, non-specific retention of the template was observed, illustrating the critical

role, which this monomer plays in the retention of the template. The effect of this reagent is not limited to the selectivity, but it also influences the morphology and the dimensions of the NPs.

3.3. Optosensing of NIF by MIP@SiC-dots.

3.3.1. Effect of pH

The recognition ability of the sensor was investigated through the changes of the fluorescence signal. The effect of pH on the fluorescence changes of sensor is given in Fig. S3 (ESM). The pH value affected not only the charge of the binding sites on MIP but also the charge of NIF. The highest fluorescence change was observed at pH 10, therefore, this pH was selected for further experiments and Britton-Robinson buffer was used to adjust the pH.

3.3.2. Effect of incubation time

The response time of the sensor for NIF was also studied. As shown in Fig. S4 (ESM), when the NIF concentration was fixed, the fluorescence intensity decreased rapidly with increasing time in the initial 10 min, after which the curve became flat. Therefore, 10 min was selected as a suitable response time for next experiments.

3.3.3. Selectivity of the imprinted sensor for NIF

The selectivity of MIP@SiC-dots was demonstrated by comparing its response to NIF with the response obtained for another dihydropyridine drug, namely NIM (Fig. 1b). As seen from Fig. 6, the fluorescence quenching constant of NIF was higher than NIM. Moreover, K_{SV} values of NIM for MIP@SiC-dots and NIP@SiC-dots are nearly the same. These results reveal that MIP@SiC-dots has a good selectivity for NIF. The well-defined structure of the imprinted cavities obviously plays an important role for rebinding of template molecules.

Furthermore, to assess the ability of the developed sensor to analyze complex real samples, the effect of some potentially interfering species on the response of the sensor was investigated. This was conducted by analyzing a solution of NIF in the presence of excess amounts of interfering compounds. The tolerance limit was taken as the concentration of the added species causing a relative error <5%. The obtained results are presented in Table 1. As seen, the amounts of most of potentially interfering species in serum and urine are below their tolerable levels or can be decreased with diluting, so there would be no interferences from these species in NIF determination.

3.3.4. Template sensing and calibration curve

The relationship between the fluorescence intensity and the concentration of NIF as a quencher can be described by the Stern–Volmer equation:

$$\frac{F_0}{F} = 1 + K_{sv}[NIF]$$

Where F_0 and F are the fluorescence intensities of the MIP@SiC-dots in the absence and presence of a given concentration of NIF, respectively and K_{SV} is the Stern–Volmer quenching constant. The Stern-Volmer plot is shown in Fig. 7. The MIP@SiC-dots exhibited linear response to NIF in the range of 0.28- 3.4 µM with a correlation coefficient (R^2) of 0.9985. The detection limit (3s) was 0.076 µM. The relative standard deviation (RSD) of 4.1 % was obtained by 5 repeated analyses of 1.0 µM solutions.

The imprinting factor (IF) is an important index to evaluate the selectivity of the imprinted materials, which is generally defined as IF = Q_{MIP}/Q_{NIP}, where Q_{MIP} and Q_{NIP} are adsorption capacity of the template on MIP and NIP, respectively. Herein, the imprinting factor can be calculated as the ratio of the Ksv value of the MIP and NIP. Under the optimum conditions, the imprinting factor was 3.28, indicating that the MIP had a much better selectivity than the NIP.

Comparison of the proposed method with some other reported analytical methods for the NIF quantification is shown in Table 2. As can be seen the developed sensor has better or comparable analytical performance compared with most of other reported methods.

To understand the fluorescence quenching due to NIF binding, some facts should be considered. The fluorescence in the SiC-dots is believed to mainly arise from radiative recombination of surface-trapped electron-hole pairs. When there is no template NIF around the MIP@SiC-dots, a blue emission is generated by exciting at 360 nm. After adding the template, the amino groups ($-NH_2$) of APTES, in binding sites of MIP@SiC-dots, can interact with the functional groups such as carbonyl in the template molecule to form a complex through hydrogen bonding[30]. So, the quenching of MIP@SiC-dots fluorescence can occur as a result of strong interaction between NIF and MIP@SiC-dots. The electron donating ability of photoexcited C-dots have well confirmed in previous works[31]. On the other hand, due to the presence of nitro group in the structure of NIF, it has a strong electron acceptor property. Therefore, it can be assumed that binding of NIF to MIP@SiC-dots facilitates the electron transfer between NIF and SiC-dots, which in turn causes a disruption to the radiative recombination of electron-hole pairs in SiC-dots. Thus fluorescence intensity decreases. On the other hand, energy transfer is not a possible mechanism for fluorescence quenching because there is no spectral overlap between the absorption spectrum of the NIF and the emission spectrum of the SiC-dots (440 nm).

3.5. Applications

To verify the applicability and validity of the presented sensor, it was applied for the determination of NIF in human serum and urine samples. Recovery studies were carried out by spiking the samples with NIF in the concentration range of 6.0-15 μM. A summary of the calculated mean NIF concentration for each sample is shown in Table 3. The obtained recoveries

are between 94.2 % and 105.6 %, which confirm the ability of our SiC-dots sensing assembly to provide accurate concentrations of NIF in biological fluids.

4. Conclusions

In this work low cost and environmentally friendly silane functionalized C-dots, having a 30% quantum yield were synthesized by means of hydrothermal decomposition of trisodium citrate in presence of an inexpensive functionalization reagent (APTES). These SiC-dots were successfully utilized as transducer to develop a MIP-coated sensor for selective recognition of NIF, for the first time. In view of the sensitivity and the selectivity, the synthesized sensor affords a very sensitive detection system for NIF analysis. The results of the fluorescent sensor for serum and urine analysis further demonstrated its feasibility for target drug recognition. Based on these observations, C-dots can be viable alternatives to traditional semiconductor quantum dots in MIP based sensors.

References

1. L.L. Brunton, J.S. Lazo and K. Parker. *Goodman & Gilman's the Pharmacological Basis of Therapics,* McGrow-Hill, New York,11th edn, 2006.

2. S.C. Sweetman, *Martindale: The Complete Drug Reference*, Pharmaceutical Press, 36th edn, 2009.

3. C.R.Galan, J.G. Álvarez, and M.V. Remolí, *Biomed. Chromatogr.,2015,* **29,** 233.

4. D. P. Patel, P. Sharma, M. Sanyal, P. Singhal, and P.S. Shrivastav, *Biomed. Chromatogr, 2012,* **26,** 1509

5. R.R. Gaichore and A.K. Srivastava, *Sensors Actuators, B,2013,* **188,** 1328.

6. L. Shang, F. Zhao and B. Zeng, *Electrochim. Acta* , 2015, **168,** 330.

7. S. Aderibigbe, O. Adegoke and O. Idowu, *Int. J. Ind. Chem., 2012,* **3,** 5.

8. B.Li, J. Xu, A.J. Hall, K. Haupt and T.S. Bui, *J. Mol. Recognit., 2014,* **27,** 559.

9. Z.H.Meng in *Molecularly Imprinted Sensors* ed. S. Songjune, Y.Ge, J.Lunec, S.A.Piletsky, Elsevier, Amsterdam, 2012.

10. W.Junping, P.Mingfei, F. Guozhen and W.Shuo, *Microchim. Acta,* **166,** 2009,295.

11. J.Zhang, Y.Niu, S. Li, R Luo and C.A.Wang, *Sensors Actuators B,* 2014, **193,** 844.

12. M.M. Moein, A. El-Beqqali, A. Abdel-Rehim, A. Jeppsson-Dadoun and M. Abdel-Rehim, *J. Chromatogr. B ,2014,* **967,** 168.

13. F.L. Dickert and O. Hayden, *Anal. Chem., 2002*,**74,** 1302.

14. S.Y. Lim, W.Shen and Z.Gao, *Chem. Soc. Rev., 2014,* **44,** 362.

15. Z.Qian, X. Shan, L. Chai, J. Ma, J. Chen and H. Feng, *ACS Appl. Mater. Interfaces*, 2014,**6,** 6797.

16. C. Liu, P. Zhang, X. Zhai, F. Tian, W. Li, J. Yong, Y.Liu, H. Wang, W. Wang, W. Liu, *Biomaterials, 2012,* **33,** 3604.

17. A. Cayuela, M.L. Soriano, M.C. Carrión and M.Valcárcel, *Anal. Chim. Acta*, *2014*, **820,** 133.

18. A. Quaranta, S. Carturan, M.Dallo Palma, M. Giarloa, N. Daldosso, G. Maggoni and G. Maritto, *Thin Solid Films*, *2014*, **553,** 188.

19. Y. Dong, R. Wang, G. Li, R. Wang, C. Chen, Y.Chi and G. Chen, *Anal. Chem., 2012,* **84,** 6220.

20. Z. Xie, F. Wang and C.Y. Liu, *Adv. Mater., 2012,* **24,** 1716.

21. F. Wang, Z. Xie, H. Zhang, C.Y. Liu and Y.G. Zhang, *Adv. Funct. Mater., 2011,* **21,** 1027.

22. H. Liu, G. Fang and S.Wang, *Biosens. Bioelectron., 2014,* **55,** 127.

23. H. Liu, D. Liu, G. Feng, F. Liu, C. Liu, Y. Yong, S. Wang, *Anal. Chim. Acta, 2013,* **762,** 76.

24. W. Zhang, X. He, Y. Chen, W.Y.Li, Y.K. Zhang, *Biosens. Bioelectron., 2011,* **26,** 2553.

25. S. Xu, H. Lu, J. Li, X. Song, A.Wang, L. Chen, S. Han, *ACS Appl. Mater. Interfaces,2013,* ,**5,** 8146.

26. Y. Mao, Y. Bao, D. Han, F. Li, and L. Niu, *Biosens. Bioelectron.,2012,* **38,** 55.

27. J. Chen, W. Liu, L.H. Mao, Y.J.Yin, C.F.Wang, S.Chen, *J. Mater. Sci.2014, **49**,* 7391.

28. W. Zhang, X.W. He, Y. Chen, W.Y. Li, Y.K.Zhang, *Biosens. Bioelectron., 2012,* **31,** 84.

29. Y. Dong, H. Li, J.Shao, Y,Chi, X. Lin, *Carbon, 2012,* **50,** 2810.

30. S. Ge, J. Lu, L. Ge, M. Yan, and j.Yu, *Spectrochim. Acta - Part A, 2011,* **79,** 1704.

31. X. Wang, L. Cao, L. Fushen, M.J. Mezaini, L. Heting, G. Qi, B. Zhou, B.A. Harruf, F. Kermarrec and Y.P. Sun, *Chem. Commun.,2009,* 3774.

32. S. M. Al-Ghannam and A.M. Al-Olyan, *Cent. Eur. J. Chem., 2008,* **6,** 222.

33. M. Baghayeri, M. Namadchian, H. Karimi-Maleh and H. Beitollahi, *J. Electroanal. Chem., 2013,* **697,** 53.

Table 1. Tolerance limits of some potentially interfering species in the determination of 300 µg L^{-1} NIF under optimum condition

Interfering species	**Tolerable concentration (mg L^{-1})**
Sucrose, Glucose, Lactose, Uric acid, Ascorbic acid, Tryptophan, Alanine, L-Cysteine, Glycine, Vitamin B1, Vitamin B2	100
Na^+, K^+, Zn^{2+}, Ca^{2+}, Cu^{2+}, Cl^-, SO_4^{2-}, Fe^{3+}	100
Cu^{2+}	5

Table2. Analytical characteristics of some published methods for determination NIF.

.**Method**	**LOD** (μM)	**Linear range** (μM)	**Ref.**
Colorimetric analysis	0.38	8-42	[7]
Spectrofluorometry	0.04	0.57-11	[32]
Voltammetry	0.72	0.8–60.0	[33]
Electrochemical sensors	0.004	0.01-4	[6]
UPLC	0.15	0.72-4	[43]
Fluorimetry	0.076	0.28-3.4	This work

Table3. Spiked Recoveries and Relative Standard Deviations (RSD, %, n = 3) in serum and urine samples using this method.

Samples	Added (μM)	Found (μM) Mean±S.D.(n=3)	Recovery (%)
Human serum	6.0	5.6±0.29	94.2
	10.0	10.4±0.96	104.2
	15.0	15.7±0.38	105.1
Urine	6.0	6.3±0.22	105.5
	10.0	9.5±0.35	94.8
	15.0	14.7±0.65	97.9

Captions for Figures

Scheme 1. Schematic illustration of the synthesis SiC-dots and MIP@SiC-dots and the sensing mechanism for NIF.

Fig. **1**. Structure of (a) Nifedipine and (b) Nimodipine.

Fig. 2 (a) TEM images of SiC-dots. (b) TEM image and (c) SEM image of MIP@SiC-dots.

Fig.3. Absorption spectrum and fluorescence spectra of SiC-dots at different excitation wavelengths.

Fig. 4. Effect of the amounts of TEOS on the imprinting factor of MIP@SiC-dots. Error bars represent standard deviation for three measurements.

Fig. 5. Effect of the amounts of APTES on the imprinting factor of MIP@SiC-dots. Error bars represent standard deviation for three measurements.

Fig.6. (a) Stern–Volmer plots for NIF using MIP@SiC-dots and NIP@SiC-dots. Error bars represent standard deviation for three measurements. (b) Fluorescence spectra of MIP@SiC-dots at different concentrations of NIF.

Fig.7. Quenching constant of MIP@SiC-dots and NIP@SiC-dots for NIF and NIM. Error bars represent standard deviation for three measurements.

Scheme 1.

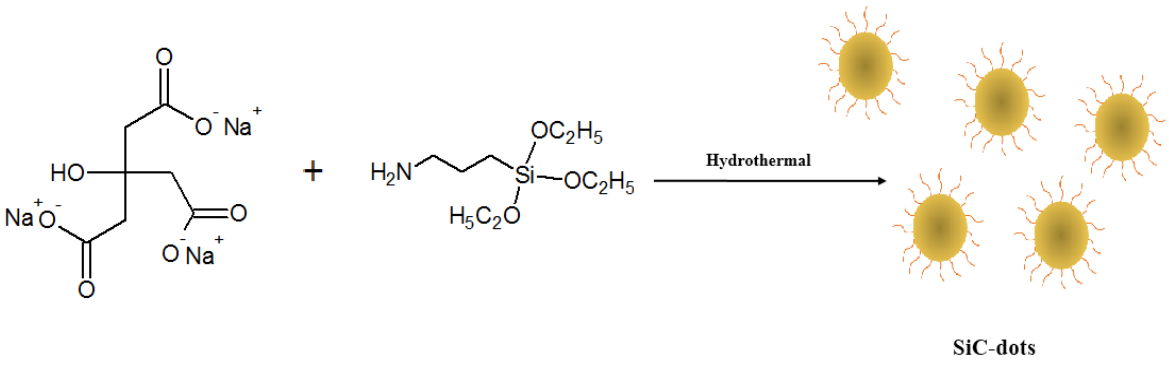

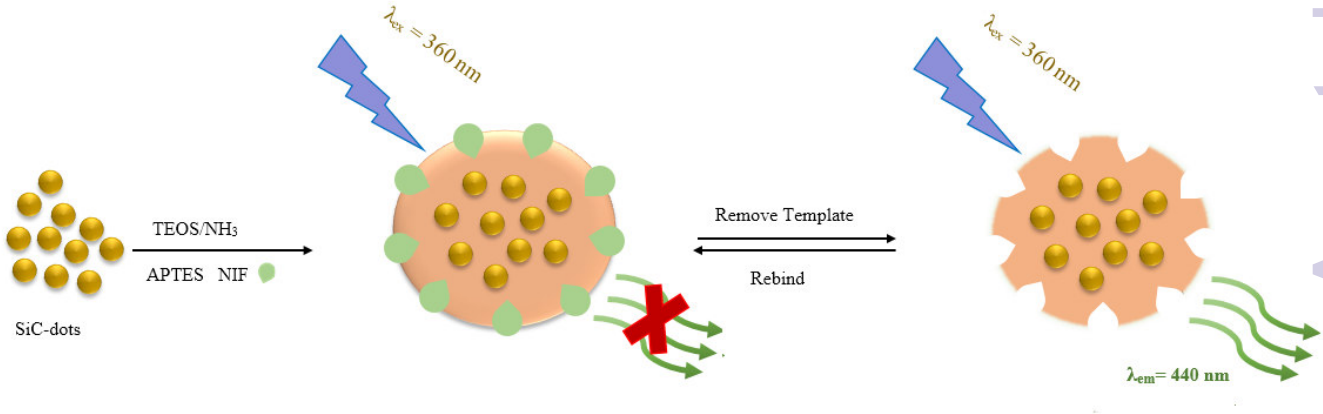

Fig. 1

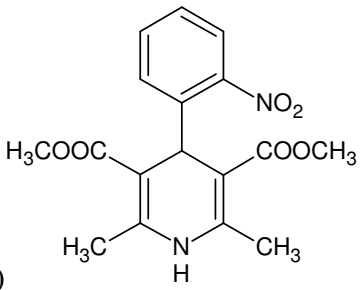

(a)

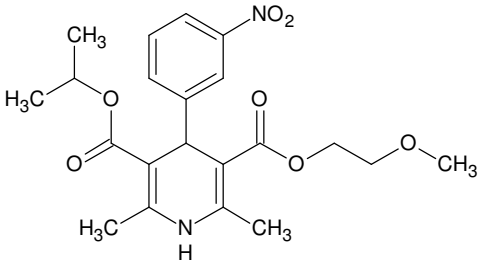

(b)

Fig.2 (a)

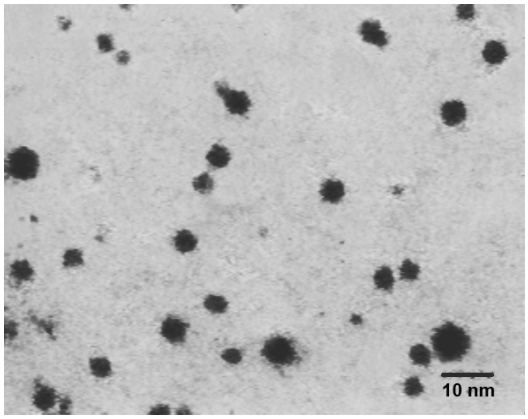

Fig.2 (b)

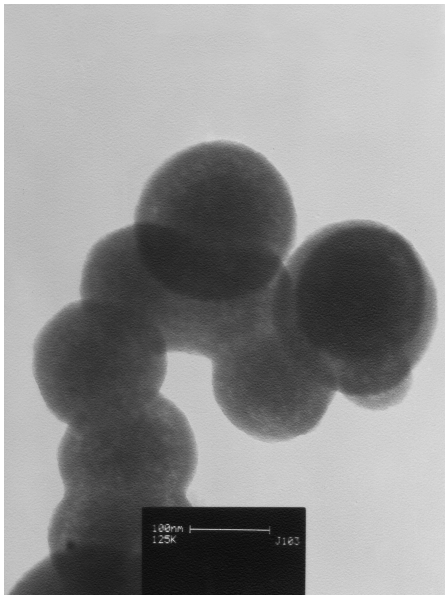

Fig.2 (c)

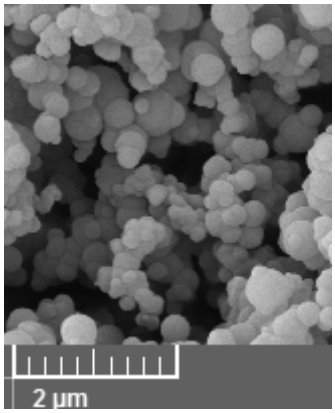

Fig.3

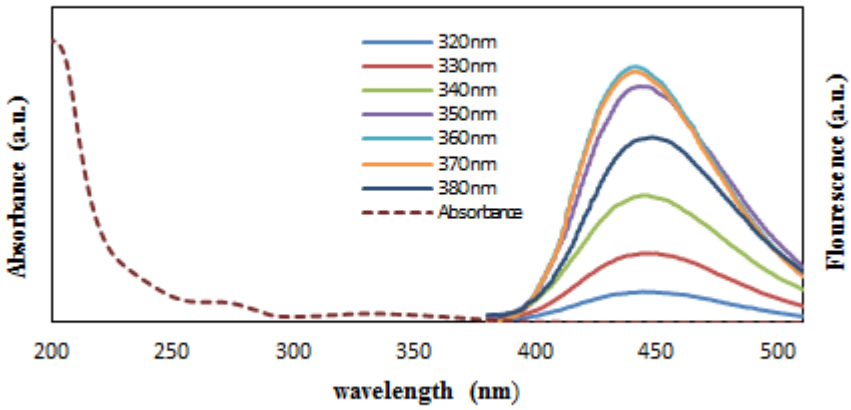

Fig.4

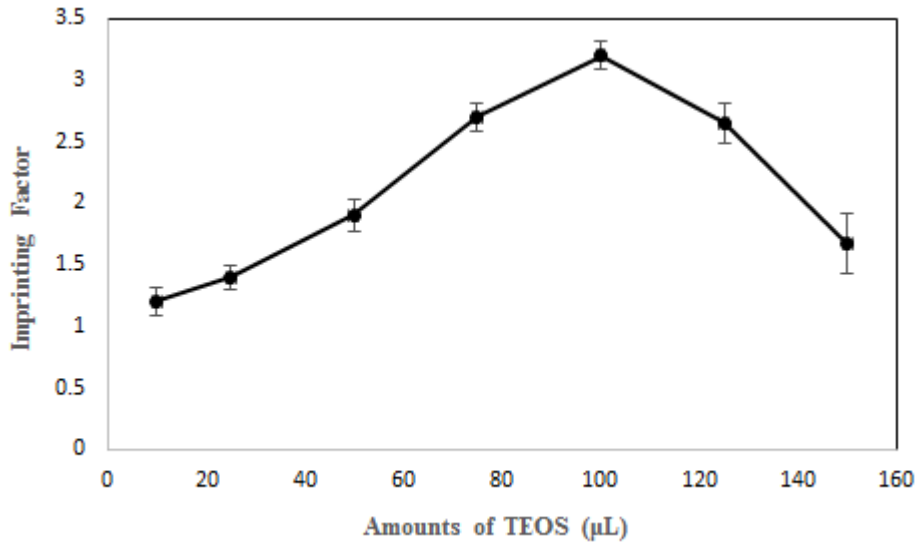

Fig.5

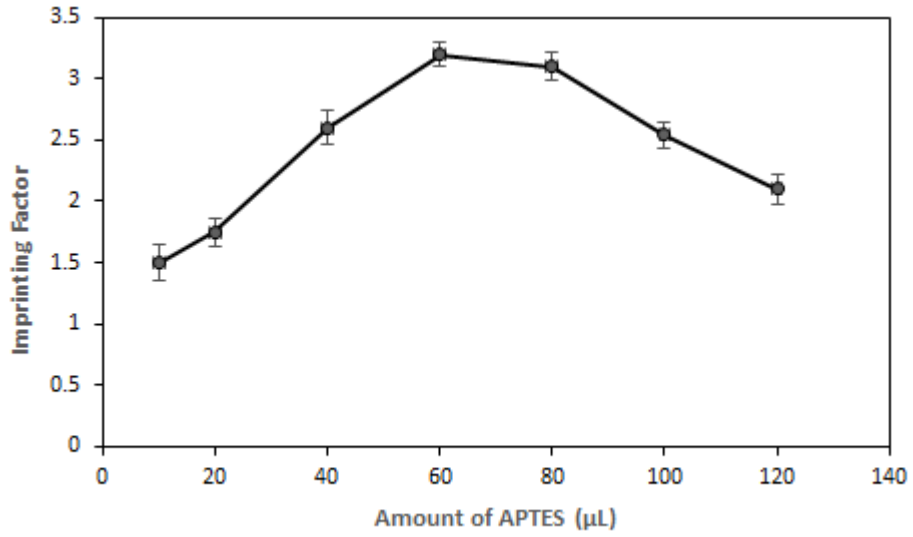

Fig.6

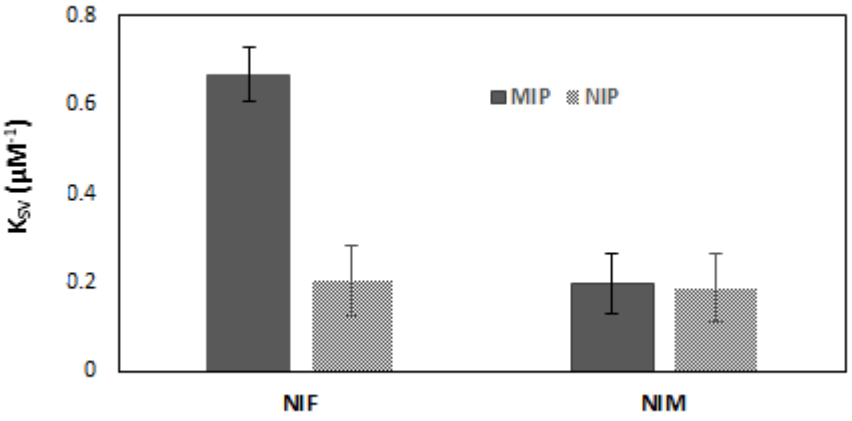

Fig.7 (a)

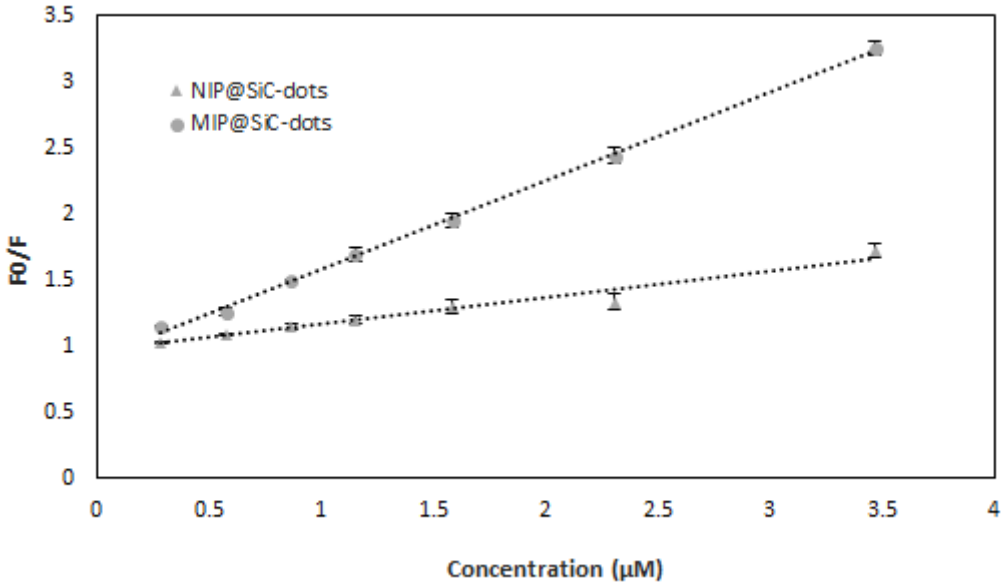

Fig.7 (b)